Journal of Computational and Applied Mathematics 291 (2016) 58–65

Contents lists available at ScienceDirect

Journal of Computational and Applied Mathematics

journal homepage: www.elsevier.com/locate/cam

A 3D mathematical model for planning ostectomy on long-bone angular deformities

L. Domenech [a,*], F.J. Muñoz-Almaraz [a], C.I. Serra [b], C. Soler [b], N. Montes [a]

[a] Escuela Superior de Enseñanzas Tecnicas, Universidad CEU Cardenal Herrera, Spain

[b] Universidad Católica de Valencia San Vicente Mártir, Facultad de Veterinaria y Ciencias Experimentales, Spain

ARTICLE INFO

Article history:
Received 15 October 2014
Received in revised form 27 March 2015

Keywords:
Corrective ostectomy
CORA
Angular deformity
3D imaging

ABSTRACT

This study describes a 3D mathematical model for planning a corrective ostectomy on long bones with angular deformities based on CT imaging. The use of three-dimensional information allows the model to compute and correct the bone angulation and rotation. The cutting point selection is developed minimizing the bone length reduction inherent in an ostectomy process. An example of its application on a two year old dog is shown at the end of the paper.

1. Introduction

Malunion after long bone fracture or abnormal growth can result in a bone deformity. This misalignment causes imbalanced joint loading and can lead to chronic pain due to ligament strain and osteoarthritis. [1]. This malunion or abnormal growth leads to a bend or break in the anatomic and mechanical axis. In order to define both axes, a mechanical axis line connects the center of a proximal joint to the center of the distal joint. An anatomic axis line is the mid-diaphyseal line, [2], which can be defined mathematically as the medial axis.

In order to measure the bone deviation, the CORA measurement (Center of Rotation of Angulation) is commonly used, [2]. It was defined as the intersection point of the proximal and distal axis line. The CORA can be found by drawing proximal and distal mechanical or anatomic axis lines, see [2]. The angle formed for both axes is the angle deformation.

Although, standard planning based on the CORA method is useful, in practice, it does not guarantee that the solution is optimal and brings forth large variation in assessing orientation parameters [3] as it is based on 2-D radiographies. Furthermore, as discussed in [4], 2-D radiographers hide a possible rotation around about the long axis of the bone, which makes impossible planning properly the rotation correction. Therefore, 3D measurement has been proven necessary for complete planning of angular deformities.

There is very little literature of studies using 3D measurements to find the optimal one-cut plane. In [5,6] a mathematical analysis of single-cut osteotomy was developed. These studies demonstrated that there is always a single-cutting plane such that, after the osteotomy a rotation of the two faces is enough to correct the whole deformation problem. However, although, in theory there is always a solution, in practice it is not always viable. In the author's own words: "When angular deformation is much greater than the torsion, the osteotomy angle approaches a plane which includes the bone axis. An excessively steep osteotomy angle resulting from little or no torsion deformity, may render this technique impractical for such cases".

* Corresponding author.
E-mail address: luis.domenech@uch.ceu.es (L. Domenech).

http://dx.doi.org/10.1016/j.cam.2015.03.058
0377-0427/

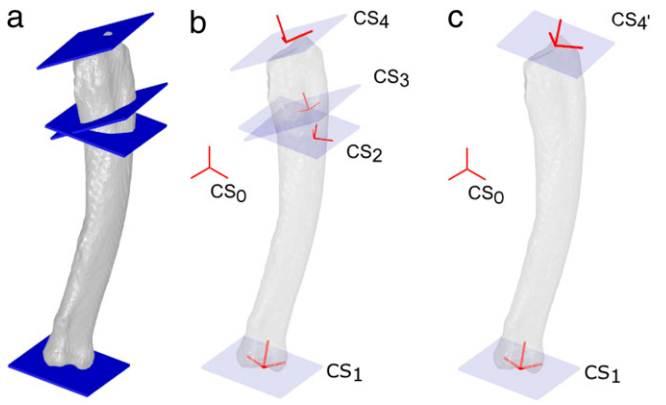

Fig. 1. (a) Joint and cutting planes. (b) Coordinate systems associated with the joint and cutting planes. (c) Coordinate systems associated with the joint planes in the correct position.

A common alternative to rotational osteotomy consists of closing wedge osteotomy, or ostectomy procedure [2]. Its main advantage is that it does not provide a unique solution, as rotational osteotomy does, but a set of solutions from which the most interesting can be selected, typically one whose cutting planes are enough orthogonal to avoid steep cutting angles. However, closing wedge osteotomy has the big disadvantage that the fragment bone is removed, which implies a length reduction. Minimizing the length reduction so that the postoperative bone is as similar as possible to the original bone is one of the objectives of this study.

Hereby, a method is presented for planning ostectomies on long bone angular deformities based on 3D CT measurements and proposes a cutting point position based on an approach of the bone length. First of all, in Section 2 a complete mathematical modeling of the osteotomy procedure is provided. Sections 2.2 and 2.3 describe the computing of the cutting plane orientations, and the estimation of the optimal cutting point respectively. Section 3 shows an example of a specific application on a 2 year old dog. The discussion is shown in Section 4.

2. Material and methods

2.1. Ostectomy mathematical model

Ostectomy procedure consists of a double-cut to the bone where the intermediate bone fragment is removed and both fragment edges are positioned to align the cutting surfaces, and rotated over the cutting planes. See Fig. 1(a).

Since the surgery procedure is composed by 3D rigid transformations, i.e. translations and rotations, it can be modeled by means of the 3D Kinematic Chain techniques. See for instance [7]. For the mathematical modeling, a local coordinate formulation based on homogeneous coordinates is provided, i.e. rotations and translations are represented by transformation matrices applied in three-dimensional homogeneous coordinates.

In the model, a coordinate system is defined at each Joint Plane (JP) and at each Cutting plane (CP). CS_1, CS_2, CS_3 and CS_4 correspond to the proximal joint plane, the proximal cutting plane, the distal cutting plane and the distal joint plane respectively. The CSs are defined such as the XY planes are the CPs or JPs, i.e., the Z axis are orthogonal to the CPs or JPs. See Fig. 1(b). The coordinates of the point P with respect to CS_i will be denoted $[P]_i$. In the same way, we denote ${}^iT_j$ as the homogeneous transformation that maps $[P]_j$ to $[P]_i$, i.e., $[P]_i = {}^iT_j \cdot [P]_j$.

The model supposes CS_1 is not centered in origin, CS_0, so that, there is a transformation in ${}^0T_1$ such as:

$$[P]_0 = {}^0T_1 \cdot [P]_1 . \tag{1}$$

On one hand, the distal pathological coordinate system CS_4 can be defined such as:

$$[P]_0 = {}^0T_1 \cdot {}^1T_4 \cdot [P]_4 \tag{2}$$

and it can also be defined fulfilling consecutive transformations:

$$[P]_0 = {}^0T_1 \cdot {}^1T_2 \cdot {}^2T_3 \cdot {}^3T_4 \cdot [P]_4 . \tag{3}$$

Combining Eqs. (2) and (3) the next relation can be obtained:

$${}^1T_4 = {}^1T_2 \cdot {}^2T_3 \cdot {}^3T_4. \tag{4}$$

On the other hand, the distal corrected bone coordinate system $CS_{4'}$ can be defined such as:

$$[P]_0 = {}^0T_1 \cdot {}^1T_{4'} \cdot [P]_{4'} \tag{5}$$

according to the reconstruction described, the corrected bone will be composed by the proximal and distal bone fragments

$$[P]_0 = {}^0T_1 \cdot {}^1T_2 \cdot {}^3T_4 \cdot [P]_{4'} \tag{6}$$

so, combining Eqs. (5) and (6), the next result can be obtained:

$${}^1T_{4'} = {}^1T_2 \cdot {}^3T_4. \tag{7}$$

Finally, any ostectomy can be modeled by means of the next equations:

$${}^1T_4 = {}^1T_2 \cdot {}^2T_3 \cdot {}^3T_4 \tag{8}$$

$${}^1T_{4'} = {}^1T_2 \cdot {}^3T_4. \tag{9}$$

Planning an ostectomy process consists of obtaining the transformations ${}^1T_2$, ${}^2T_3$ and ${}^3T_4$ based on the information of the pathological bone, ${}^1T_4$, and the desired configuration, ${}^1T_{4'}$. The positions and orientations of the CP can be easily obtained with these values. Nevertheless, it is not possible to obtain a unique solution for ${}^1T_2$, ${}^3T_4$ and ${}^2T_3$ from Eqs. (8) and (9), as given any transformation ${}^1T_2$, ${}^2T_3$ and ${}^3T_4$ is determined by (10) and (11).

$${}^3T_4 = \left({}^1T_2\right)^{-1} \cdot {}^1T_{4'} \tag{10}$$

$${}^2T_3 = \left({}^1T_2\right)^{-1} \cdot {}^1T_4 \cdot \left({}^1T_{4'}\right)^{-1} \cdot {}^1T_2. \tag{11}$$

Although, the previous model is completely based on values of ${}^1T_4$ and ${}^1T_{4'}$, these values are not always known, ${}^1T_{4'}$ is a theoretical hypothesis that is not always accomplished. The reason being that the position of $CS_{4'}$ cannot be fixed since some values imply an open-wedge osteotomy, which is outside the objective of this study. However, the orientation of ${}^1T_{4'}$ can actually be fixed which is the main objective of the procedure, so orientation and position are studied separately.

2.2. Rotation formulation

According to the Homogeneous Coordinates Transformation properties, the following equations can be obtained based on (10) and (11):

$${}^3R_4 = \left({}^1R_2\right)^{-1} \cdot {}^1R_{4'} \tag{12}$$

$${}^2R_3 = \left({}^1R_2\right)^{-1} \cdot {}^1R_4 \cdot \left({}^1R_{4'}\right)^{-1} \cdot {}^1R_2 \tag{13}$$

where ${}^iR_j$ corresponds to the rotation matrix corresponding to the transformation ${}^iT_j$.

Remark 1. The matrix ${}^2R_3$ is similar to the product ${}^1R_4 \cdot \left({}^1R_{4'}\right)^{-1}$ with ${}^1R_2$ being the change of basis matrix. If ${}^1R_2$ is selected then ${}^2R_3$ is a rotation over the z-axis, both CS_2 and CS_3 will be equal but a z-axis rotation, so both XY-planes will be parallel.

It implies the intermediate fragment has zero size and it would be the case of a rotational osteotomy. In this sense, a rotational osteotomy can be understood as a degenerate case of an ostectomy [6].

2.3. Optimal cutting point

As it has been explained, the position of the Distal CS cannot directly be fixed, however, a valid criterion based on surgical reasons consists on minimizing the bone removing, understood as the bone length. In this section a length modeling for single-level angular deformity is provided.

To start with the optimization process, the solution space must be determined. In our case, the cutting axis is defined as the intersection of the cutting planes, and the cutting point is defined as the intersection of the bone surface and the cutting axis. Fig. 2 shows the different relative positions of the cutting axis and the bone surface. The importance of the relative positions lies in that only tangent cutting axis is valid in the ostectomy procedure. On the one hand, internal positions are avoided because they produce 2 intermediate fragments and 2 cut surfaces in proximal and distal fragments. That configuration makes the reduction and alignment during the surgery execution impractical. On the other hand, external positions produce bigger intermediate fragments, increasing the bone length reduction which is contrary to our purpose. Based on this analysis, the solution space for the cutting point optimization is defined as the set of points γ of the bone surface tangent to the cutting axis. In the Appendix is proved γ to be a non-empty continuous one-dimension space. Under this condition, γ can be described as a 3D curve $\vec{r}\,(s)$ where s is the natural parameter of the curve. See Fig. 3(b).

The bone length is a complex concept, specially at angulation deformed bones. In this study the postoperative bone length is obtained by the sum of the fragment length projections to the orthogonal axis of its respective joint plane. See Fig. 3(a). The definition corresponds to the distance between the joint planes in a parallel situation and it is a good estimation under the hypothesis of single-level deformity.

$$L_T\left(\vec{r}\,(s)\right) = L_{1,2}\left(\vec{r}\,(s)\right) + L_{3,4}\left(\vec{r}\,(s)\right) \tag{14}$$

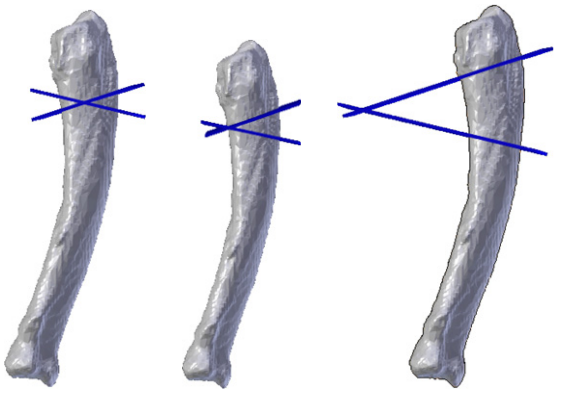

(a) Secant position. (b) Tangent position. (c) External position.

Fig. 2. Relative positions of the bone and the cutting axis, represented by the intersection of the cutting planes.

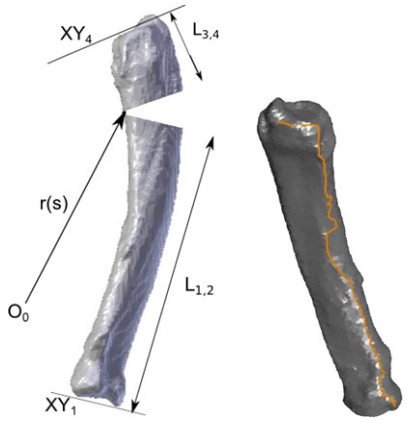

(a) Obtaining the total length of the reconstructed bone. (b) Representation of the curve γ.

Fig. 3. Cutting point position.

where $L_{1,2}$ and $L_{3,4}$ are defined as the lengths of the fragments closer to the proximal and distal joint, respectively.

$$L_{1,2}\left(\vec{r}\,(s)\right) = \left(\vec{r}\,(s) - \vec{O}_1\right) \cdot \vec{Z}_1 \tag{15}$$

$$L_{3,4}\left(\vec{r}\,(s)\right) = \left(\vec{O}_4 - \vec{r}\,(s)\right) \cdot \vec{Z}_4 \tag{16}$$

where $\vec{Z}_1$ and $\vec{Z}_4$ are the third axis unit vector in the CS_1 and CS_4 respectively, orthogonal to the Joint Planes, and $\vec{O}_1$ and $\vec{O}_4$ are the origin of CS_1 and CS_4 respectively.

In order to start with the optimization process, the critical points are calculated:

$$\frac{dL_T\left(\vec{r}\,(s)\right)}{ds} = 0 \tag{17}$$

by using the linearity property and the chain rule, this can be written as:

$$\left(\nabla L_{1,2}\left(\vec{r}\right) + \nabla L_{3,4}\left(\vec{r}\right)\right) \cdot \frac{d\vec{r}}{ds} = 0. \tag{18}$$

By definition, the derivative of the parameterization with respect the natural parameter, $d\vec{r}/ds$, is the unitary tangent vector to the curve γ and it is denoted by $\vec{T}$ for now on. The gradients of the functions $L_{1,2}$ and $L_{3,4}$ are the vectors $\vec{Z}_1$ and $-\vec{Z}_4$ respectively.

$$\frac{d\vec{r}}{ds} = \vec{T} \tag{19}$$

$$\nabla L_{1,2}\left(\vec{r}\right) = \vec{Z}_1 \tag{20}$$

$$\nabla L_{3,4}\left(\vec{r}\right) = -\vec{Z}_4 \tag{21}$$

where $\vec{T}$ is the unitary tangent vector. Then, Eq. (18) can be expressed in this way:

$$\left(\vec{Z}_1 - \vec{Z}_4\right) \cdot \vec{T} = 0. \tag{22}$$

By definition, $\vec{Z}_1, \vec{Z}_4$ and $\vec{T}$ are unitary vectors, so that the product will be 0 if the vectors are orthogonal. Then, the critical points C fulfill the following geometrical condition:

$$\left(\vec{Z}_1 - \vec{Z}_4\right) \perp \vec{T}\,(C)\,. \tag{23}$$

According to the **Second derivative test**, a critical point is a local maximum if its second derivative is negative.

$$\frac{d^2 L_T\left(\vec{r}\,(s)\right)}{ds^2} < 0 \tag{24}$$

$$\frac{d^2 L_T\left(\vec{r}\,(s)\right)}{ds^2} = \left(\vec{Z}_1 - \vec{Z}_4\right) \cdot \frac{d\vec{T}\ (s)}{ds} < 0. \tag{25}$$

Applying the definition of curvature:

$$\frac{d\vec{T}\ (s)}{ds} = \kappa\,(s)\,\vec{N}\,(s) \tag{26}$$

where $\kappa\,(s)$ and $\vec{N}\,(s)$ are the curvature and the normal vector respectively. So that:

$$\frac{d^2 L_T\left(\vec{r}\,(s)\right)}{ds^2} = \left(\vec{Z}_1 - \vec{Z}_4\right) \cdot \left(\kappa\,(s)\,\vec{N}\,(s)\right) < 0. \tag{27}$$

The result of a scalar product is negative if the angle between both vectors is greater than the right angle.

In the case that the angle is exactly $\frac{\pi}{2}$, or $\kappa\,(s) = 0$, the critical point can be determined using higher derivatives. If more than one point fulfills the described conditions, the objective function is evaluated at all of them and the point with the greatest value is selected.

3. Example of application

As an example of a specific application, a 2 years old male afghan hound dog is presented. Fig. 4 shows the right foreleg radio-ulnar angular deformity.

The JPs were performed by isolating anatomical landmarks in a similar way to [8]. CSs were defined such as Z axis is orthogonal to the JPs and Y axis corresponds to the cranial direction. The procedure selected for the cutting described has been applied using a parallel planes strategy, i.e., the cutting planes have been chosen parallel to the joint planes. This strategy guarantees transversal cutting planes and avoids to perform steep cuts.

The process has been developed as follows:

- Obtain the three-dimensional data of the pathological bone by means of CT scan.
- Determine the Joint Planes.
- Choose the Rotation matrix ${}^1R_2$ by means of a parallel strategy, obtaining the orientation of CS_2 parallel to CS_1.
- Using (12) and (13) obtain the orientation of CS_3.
- Determine the Optimal Cutting Point in the bone surface, based on (23) and (27).

However, as explained in [9], applying the computed cutting planes position and orientation accurately during the intervention remains a challenge to the surgeon. The methodology explained in [10] has been applied to design a customized device to assist the surgeon in performing the operation as similar as possible to the computed solution. The designed device, manufactured by means of rapid prototyping technology, incorporates 2 cutting guides that indicates the position and orientation where the cuts to the surgeon. Furthermore, the designed device has two marks on each edge of the bone fragments which allow the surgeon not only the alignment of both cutting surfaces but also the rotation until marks match assuring the correct alignment of CS_2 and CS_3. Fig. 5 shows the planned ostectomy with the bone 3D model. Fig. 6 shows the developed device and its bone compatibility. Finally, Fig. 7 shows the post-operative radiological analysis.

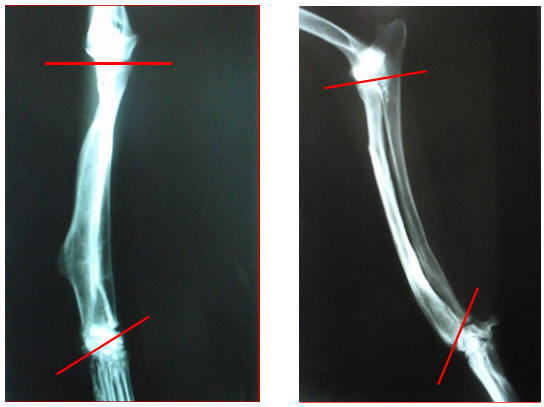

Fig. 4. Radio-ulnar angular deformity. AP and medio-lateral pre-operative radiologic analysis.

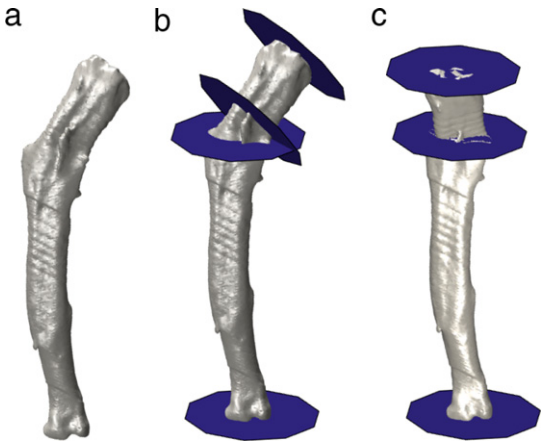

Fig. 5. 3D images showing the planning method. (a) Shows the 3D bone model. (b) Shows the joint planes and the obtained cutting planes. (c) Shows the forecast of the reconstructed bone after alignment and rotation.

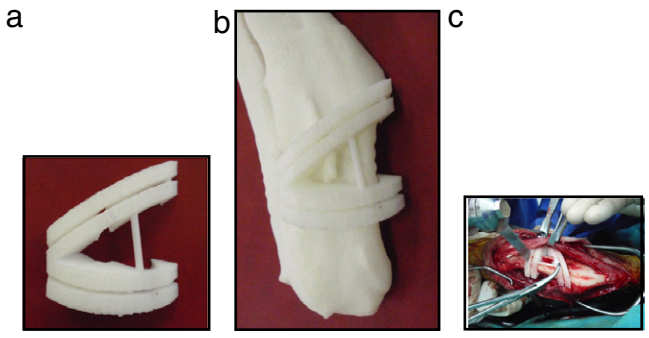

Fig. 6. The patient-specific designed device in the "in vitro" and "in vivo" stages. (a) Designed device with the slots for guiding the saw to the correct CP. (b) Designed device fixed in a rapid prototyping based bone reconstruction. (c) Designed device fixed to the real bone in the operating room.

4. Discussion

This study describes a mathematical model for planning ostectomies for angular deformities on long bones. In this method, the 3D information of the pathological bone is required as well as a reference to the correct alignment that the bone should be. Closing wedge osteotomy is a common option in angular deformities correction, and can be an interesting alternative when rotational osteotomy planning produces a very steep cutting plane or a large rotation angle. This occurs in cases where the angulation is bigger than the rotation, or the rotation angle reduces the contact area more than the recommended value [4].

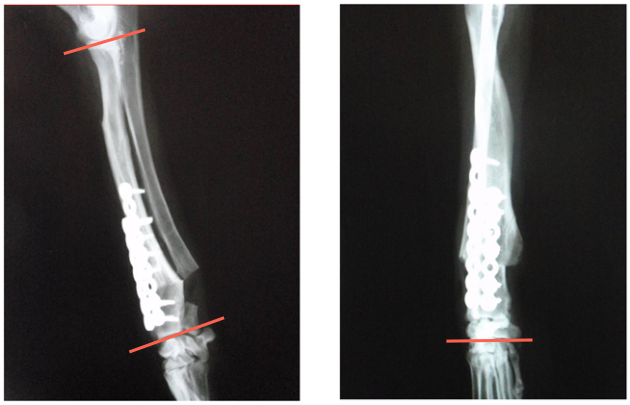

Fig. 7. Anterior–posterior and medio-lateral post-operative radiology analysis.

In this case, the proposed method provides a set of solutions for the orientation of the cutting planes, allowing the surgeon to select the most interesting according to the bone characteristics. It also allows the surgeon to avoid steep cutting planes or insufficient contact area.

However, the closing wedge osteotomy has a drawback. Closing wedge osteotomy procedure removes a bone fragment, which reduces the total bone length. Depending on the bone an excessive length reduction could produce other malfunctions. In order to reduce these problems, an optimal cutting point has been proposed. Its computation is based on an approximation of the length bone definition that coincides with the joint planes distance in the case of parallel planes. The selected point cannot be assured to avoid length reduction problems, and it depends on the bone characteristics and the selected cutting orientation planes.

The mathematical model proposed has been developed for single-level angular deformities. Nevertheless, it can be extended to multi-level angular deformities adding more CP and their correspondent CS. The definition of bone length must be reconsidered in the case of three or more fragments since the length is computed as the projection to the orthogonal axis of its respective JP, and the intermediate fragments do not have JP.

Appendix. Unidimensional and continuous proof of the solution space

Let $\vec{L}$ be a vector called the cutting axis direction.

We now focus on the study of the set γ of points, such that the vector $\vec{L}$ is tangent to the bone surface. In this section, we prove that set γ is a non-empty set and that under generic conditions set γ is a regular curve.

Let $B(u, v)$ be a regular parameterization of the deformed bone surface and $P_0 = B(u_0, v_0)$ a point of γ. We assume that the bone surface is holomorphic to a sphere.

Let $\vec{N}$ be a vector field on the bone surface, where $\vec{N}$ is the unitary exterior normal vector to the surface and $\vec{R}$ a constant vector orthogonal to $\vec{L}$. There exists a point on the bone surface where the vector field $\vec{N} \times \vec{R}$ is the vector zero. Otherwise, the vector field $\vec{N} \times \vec{R}/\|\vec{N} \times \vec{R}\|$ would be a non-vanishing continuous tangent vector field that contradicts the "hairy ball theorem" [11]. At the point where $\vec{N} \times \vec{R} = \vec{0}$ the vector $\vec{L}$ is orthogonal to $\vec{N}$. Therefore, $\vec{L}$ is tangent at least to one point in the bone surface and then γ is a nonempty set.

Proposition 1. *Under the above assumptions, if the normal curvature in the direction $\vec{L}$ is not null ($\kappa(\vec{L}) \neq 0$), there exists a neighborhood of P_0 such that γ is a regular curve, i.e. there exists a one-dimensional parameterization of γ.*

Proof. The vector $B_u \times B_v$ is not null and normal to the surface B, since it is a regular parameterization of the bone. A point of the set γ is characterized by the cutting axis $\vec{L}$ being orthogonal to the vector $B_u \times B_v$. Therefore, a function F is defined such that its zero level is the set γ.

$$F(u, v) = (B_u \times B_v) \cdot \vec{L}. \tag{A.1}$$

In the following, the objective consists in proving that the function $F(u, v)$ verifies the conditions of the **implicit function theorem**, namely, the function vanishes at (u_0, v_0) and one of its partial derivatives is not null at the point.

Taking derivative of this function

$$\nabla F = \begin{bmatrix} (B_{uu} \times B_v + B_u \times B_{uv}) \cdot \vec{L} \\ (B_{uv} \times B_v + B_u \times B_{vv}) \cdot \vec{L} \end{bmatrix}. \tag{A.2}$$

Since $\vec{L}$ is tangent to the surface at P_0, it can be written as a linear combination of the basis vectors of the tangent plane B_u^0 and B_v^0. Hence, there exist α_0 and β_0 such that $\vec{L} = \alpha_0 B_u^0 + \beta_0 B_v^0$ where $B_u^0 = B_u(u_0, v_0)$, $B_v^0 = B_v(u_0, v_0)$ and analogous notation for second order partial derivatives. The gradient of the function F at the point (u_0, v_0) is

$$\nabla F^0 = \begin{bmatrix} \alpha_0(B_{uu}^0 \times B_v^0) \cdot B_u^0 + \beta_0(B_u^0 \times B_{uv}^0) \cdot B_v^0 \\ \alpha_0(B_{uv}^0 \times B_v^0) \cdot B_u^0 + \beta_0^0(B_u^0 \times B_{vv}^0) \cdot B_v \end{bmatrix}. \tag{A.3}$$

By definition of the unitary normal vector to a surface, this vector is proportional to the vector product $B_u^0 \times B_v^0$, i.e., $B_u^0 \times B_v^0 = \lambda \vec{N}_0$ where $\lambda = \|B_u^0 \times B_v^0\|$. Using that definition and the scalar triple product properties, the scalar triple products in (A.3) are:

$$\begin{aligned}
(B_{uu}^0 \times B_v^0) \cdot B_u^0 &= -(B_u^0 \times B_v^0) \cdot B_{uu}^0 = -\lambda \vec{N}_0 \cdot B_{uu}^0 \\
(B_u^0 \times B_{uv}^0) \cdot B_v^0 &= -(B_u^0 \times B_v^0) \cdot B_{uv}^0 = -\lambda \vec{N}_0 \cdot B_{uv}^0 \\
(B_{uv}^0 \times B_v^0) \cdot B_u^0 &= -(B_u^0 \times B_v^0) \cdot B_{uv}^0 = -\lambda \vec{N}_0 \cdot B_{uv}^0 \\
(B_u^0 \times B_{uv}^0) \cdot B_v^0 &= -(B_u^0 \times B_v^0) \cdot B_{vv}^0 = -\lambda \vec{N}_0 \cdot B_{vv}^0.
\end{aligned}$$

The gradient of the function F at the point (u_0, v_0) is rewritten as follows:

$$\begin{aligned}
\nabla F(u_0, v_0) &= -\lambda \begin{bmatrix} \alpha_0 \vec{N}_0 \cdot B_{uu} + \beta_0 \vec{N}_0 \cdot B_{uv} \\ \alpha_0 \vec{N}_0 \cdot B_{uv} + \beta_0 \vec{N}_0 \cdot B_{vv} \end{bmatrix} \\
&= -\lambda \begin{bmatrix} \vec{N}_0 \cdot B_{uu} & \vec{N}_0 \cdot B_{uv} \\ \vec{N}_0 \cdot B_{uv} & \vec{N}_0 \cdot B_{vv} \end{bmatrix} \begin{bmatrix} \alpha_0 \\ \beta_0 \end{bmatrix}.
\end{aligned}$$

Therefore, the scalar product $(\alpha_0, \beta_0) \cdot \nabla F(u_0, v_0)$ is λ multiplied by the second fundamental form (see for instance [12] for the definition of the second fundamental form) of the bone in the direction $\vec{L}$.

$$(\alpha_0, \beta_0) \cdot \nabla F(u_0, v_0) = -\lambda \mathbb{I}(\vec{L}). \tag{A.4}$$

The normal curvature of B in the direction $\vec{L}$ is the quotient of the second and first fundamental forms in the direction $\vec{L}$, $\kappa(\vec{L}) = \mathbb{I}(\vec{L})/\mathrm{I}(\vec{L})$. Consequently,

$$(\alpha_0, \beta_0) \cdot \nabla F(u_0, v_0) = -\lambda \, \kappa(\vec{L}) \, \mathbb{I}(\vec{L}). \tag{A.5}$$

This expression is different from zero. Indeed, the normal curvature is not null and, for a regular parameterization, the factors $\lambda = \|B_u^0 \times B_v^0\|$ and $\mathbb{I}(\vec{L})$ are not zero. Hence, the factor $\nabla F(u_0, v_0)$ in the scalar product cannot be the zero vector and at least one of the partial derivatives of F is not null, suppose v. The function F meets the conditions of the **implicit function theorem** and there exists a function $v(u)$ such that $(u, v(u))$ is the set of zero level of F. □

Remark 2. In the case of parabolic points (one of the principal curvature is zero), the conditions of the proposition are not fulfilled if the vector $\vec{L}$ is in the direction of the null eigenvector of the matrix of the second fundamental form. For instance, if the bone is a cylinder and the cutting axis is in the direction of the generatrix, the set γ is not one-dimensional but the whole bone.

References

[1] S.A. Milner, T.R.C. Davis, K.R. Muir, D.C. Greenwood, M. Doherty, Long-term outcome after tibial shaft fracture: is malunion important? J. Bone Joint Surg. [Am.] 84-A (6) (2002) 971–980.
[2] M.D.F. Dror Paley, Principles of deformity correction, in: Skeletal Trauma, Vol. 63, fourth ed., Saunders, 2009, (Chapter).
[3] K. Thomason, K.L. Smith, The reliability of measurements taken from computer-stored digitalised x-rays of acute distal radius fractures, J. Hand Surg. Eur. 33 (3) (2008) 369–372.
[4] J.G.G. Dobbe, K.J.d. Pré, P. Kloen, L. Blankevoort, G.J. Streekstra, Computer-assisted and patient-specific 3-d planning and evaluation of a single-cut rotational osteotomy for complex long-bone deformities, Med. Biol. Eng. Comput. 49 (12) (2011) 1363–1370.
[5] B.J. Sangeorzan, B.P. Sangeorzan, S.T. Hansen Jr., R.P. Judd, Mathematically directed single-cut osteotomy for correction of tibial malunion, J. Orthop. Trauma 3 (4) (1989) 267–275.
[6] B.P. Sangeorzan, R.P. Judd, B.J. Sangeorzan, Mathematical analysis of single-cut osteotomy for complex long bone deformity, J. Biomech. 22 (11–12) (1989) 1271–1278.
[7] J.M. McCarthy, Introduction to Theoretical Kinematics, 1990.
[8] K.R. Crosse, A.J. Worth, Computer-assisted surgical correction of an antebrachial deformity in a dog, Vet. Comp. Orthop. Traumatol. 23 (5) (2010) 354–361.
[9] D.C. Meyer, K.A. Siebenrock, B. Schiele, C. Gerber, A new methodology for the planning of single-cut corrective osteotomies of mal-aligned long bones, Clin. Biomech. (Bristol, Avon) 20 (2) (2005) 223–227.
[10] L. Domenech, C. Soler, J. Soriano, V. Moratalla, C. Serra, Development of a custimized device for correction of angular deformities of long bones in small animals. A case report, in: A. Vezzoni, E. Taravella (Eds.), 17th ESVOT Congress Venice. No. 17, ESVOT, Venice Lido, October 2–4, 2014.
[11] J. Milnor, Analytic proofs of the" hairy ball theorem" and the brouwer fixed point theorem, Amer. Math. Monthly (1978) 521–524.
[12] A. Gray, Modern Differential Geometry of Curves and Surfaces, in: Studies in Advanced Mathematics, CRC Press, 1993.